Improving applied roughness measurement of involute helical gears

G Koulin, J Zhang, RC Frazer, SJ Wilson and BA Shaw
Design Unit, School of Mechanical and Systems Engineering, Newcastle University, Newcastle upon Tyne, NE1 7RU, United Kingdom

E-Mail: giorge.koulin@ncl.ac.uk

Abstract. With improving gear design and manufacturing technology, improvement in metrology is necessary to provide reliable feedback to the designer and manufacturer. A recommended gear roughness measurement method is applied to a micropitting contact fatigue test gear. The development of wear and micropitting is reliably characterised at the sub-micron roughness level. Changes of the localised surface texture features are revealed and are related to key gear meshing positions. The application of the recommended methodology is shown to provide informative feedback, to the gear designer, in reference to the fundamental gear coordinate system which is used in gear performance simulations such as tooth contact analysis.

PACS: 06.20.Dk; 46.50.+a

Keywords: roughness measurement, gear surface texture, contact fatigue testing, involute gears, micro pitting

1 Introduction

Modern high power gear transmissions requires the highest quality design, manufacturing and measurement engineering processes. A gear designer optimises the theoretical gear design within the limits of the manufacturing processes available to them. During and post manufacturing, various metrological checks are used to verify the manufactured gear quality satisfies the design requirements. Amongst various checks performed are form, topography and roughness measurements [1]. The form and waviness of a gear flank is typically characterised by a dedicated gear measurement machine (GMM), which measures relative to an unmodified involute geometry, providing measurement results in the gear coordinate system. Material gear testing is also required in order to establish endurance limits of the material with respect to primary failure modes such as micropitting [2]. Micropitting is a contact fatigue failure mode that can cause excessive noise and vibration during gear operation and lead to other failure modes such as macro pitting or flank bending failures. The depth and extent of micropitting damage is typically quantified by similar metrological checks that are used in the manufacturing stages.

Roughness of the surface influences friction coefficient, lubrication conditions and therefore performance with respect to efficiency, contact fatigue failure modes and other useful operating parameters [3]. Therefore roughness measurements can be used to verify the quality of the manufactured gear as well as to monitor the progression of wear and development of failure [4, 5].

The usefulness of roughness measurement in gears is clearly seen. However the guidelines given by geometric specification standards and codes of inspection practices on how to measure gear surface texture are not well defined.

A new approach to roughness measurement recommends a more robust definition of the gear roughness measurement method, described in [6], that better represents the functional (meshing action) of the gears during operation. The method allows repeatable measurements to be made on a gear flank from root to tip. The method uses a fixture to define the measurement relative to the gear coordinate system, which is useful in order to make comparison with design intent at key meshing positions. The repeatability of this method allows the monitoring of the progression of wear and micropitting of the flank, identifying changes of the local surface features as the damage progresses.

An application of this new gear roughness measurement approach is presented in this paper. The method is used to monitor progression of wear and micropitting on a pair of test gears following BGA-DU (British Gear Association) micropitting test procedure [7]. The method is used to quantify surface texture parameter changes and also how localised features change, at the roughness level, as the gears are manufactured, initially run in and then load tested to induce micro pitting damage.

2 Methodology

A pair of involute helical test gears was tested with the objective of developing wear and micropitting on the active gear flanks. The gears are measured prior to testing and after each stage of the test. These interval measurements are used to monitor the progression of wear and micropitting on the gear flanks.

A Form Talysurf Intra 50 shop floor roughness profiler instrument is used to measure the gears. A long series probe is used to increase the amplitude range with a 2µm radius 90° conical diamond tip. The longer probe is necessary to span part of the gear root region, the highest point on the flank and the tip of the gear tooth. The amplitude resolution of the system is 32 nm. All measurements were taken at the stylus speed of 0.5 mm/s with lateral point sampling of 0.5 µm. The measurement uncertainty of this shop floor machine was assessed following the guidelines in the references [8, 9].

The gear is located in reference to the profiler axis with a fixture, which is illustrated in Figure 1 and described in detail in the reference [6]. The fixture provides a rigid mounting which can be replicated closely at each measurement interval. Measurements can be made in a similar position which enables the progressive monitoring of the surface features as testing proceeds.

The measured profiles are treated in accordance with the previously published methodology [6]:

1. A mathematical model of the involute gear geometry is constructed.
2. A theoretical measurement plane is orientated in such a way so as to reflect the physical orientation of the profiler with respect to the gear.

3. The intersection between the involute gear geometry surface and the theoretical measurement plane defines a line. This line represents the form of the nominal gear surface as would be measured by a theoretical profiler.
4. The theoretical form trace is aligned to and subtracted from the measured trace of the test gear, revealing the surface texture features.

Comparison between the as manufactured, run in and after testing conditions of the surface is made. General surface roughness parameters are also calculated and compared.

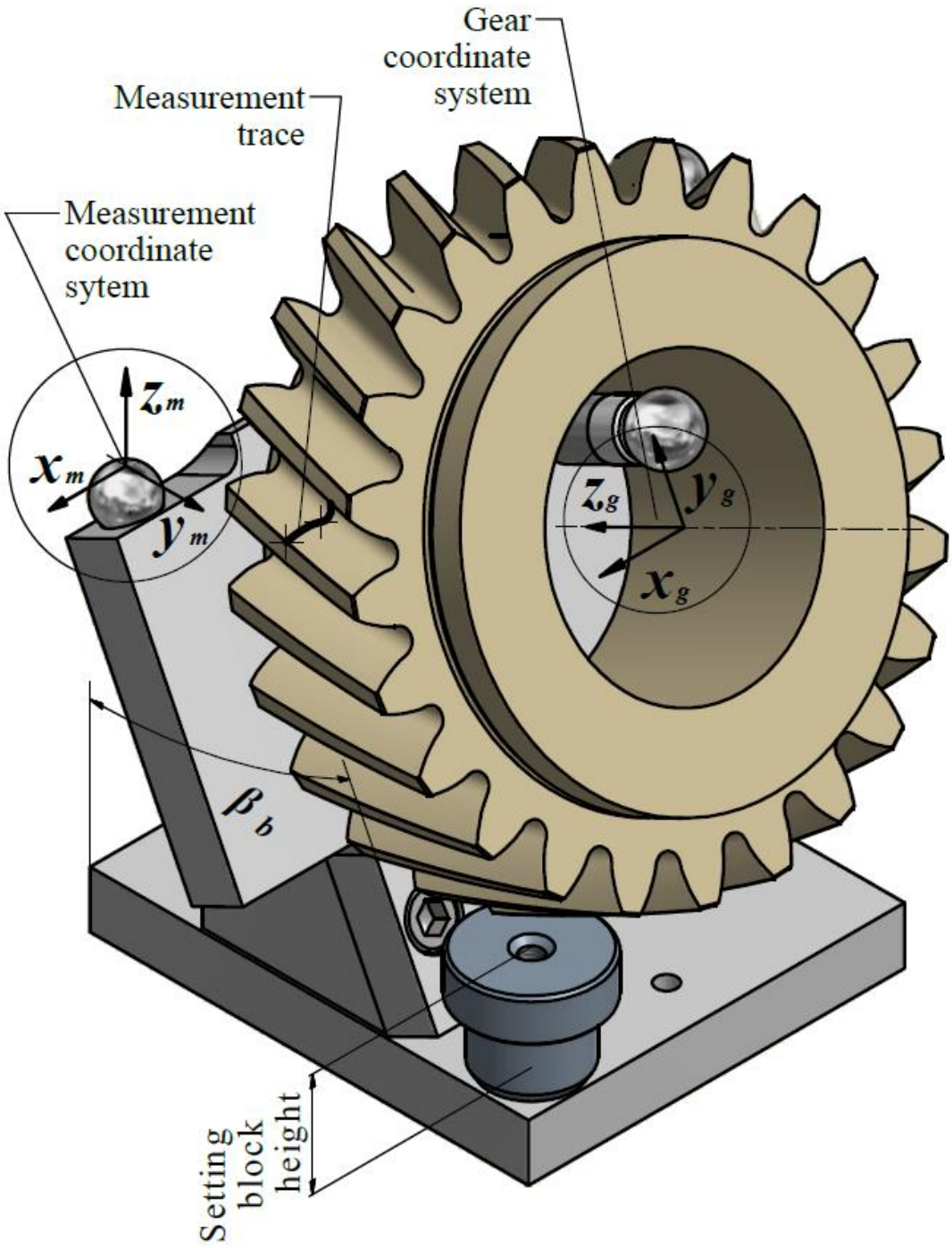

Figure 1: Gear alignment fixture CAD model as illustrated in reference [6].

2.1 Gear geometry

The gear test follows the BGA-DU micropitting test procedure, for 160 mm centre distance gear pairs. The key geometry parameters for the test gear pair are summarised in Table 1. In addition, the key positions that define changes in the contact conditions, as the gear pair rotate in mesh, are defined:

- Start and end of active profile (SAP and EAP) mark positions of tooth engaging and disengaging contact.

- Lowest and highest points of single tooth contact (LPSTC and HPSTC) marks beginning and end of a region in which only a single tooth of each gear are contacting in the transverse plane.
- Pitch point of the meshing gear pair marks the point at which the gears are in pure rolling. The sliding between the gear teeth in contact increases further away from the pitch line.

These positions are labelled from A to E. An illustration to aid understanding is shown in Figure 2. Additionally the gear design uses a 'long tip relief strategy', meaning that the start of tip relief of pinion meshes with the positions of LPSTC of the wheel and vice versa. The start of linear tip relief creates a discontinuity on the gear surface that can promote micropitting damage.

Table 1: Nominal involute helical test gear pair geometry parameters.

Parameter	Pinion	Wheel
Number of teeth	23	24
Normal module (mm)	6	
Face width (mm)	44	
Reference pressure angle (°)	20	
Reference helix angle (°)	28.1	
Base helix angle (°)	26.27	
Centre distance (mm)	160	
Hand of helix	(-ve) left	(+ve) right
Root diameter (mm)	139.697	146.444
Base diameter d_b (mm)	144.614	150.901
Start of active profile (SAP) diameter A (mm)	148.481	155.083
Lowest point of single tooth contact (LPSTC) diameter B (mm)	152.212	158.841
Pitch line of the meshing gears diameter C (mm)	156.596	163.404
Highest point of single tooth contact (HPSTC) diameter D (mm)	162.072	168.634
Tip diameter or end (mm) of active profile (EAP) E (mm)	168.664	175.103
Start of tip relief diameter (mm)	162.072	168.634
Linear tip relief C_α (µm)	50	

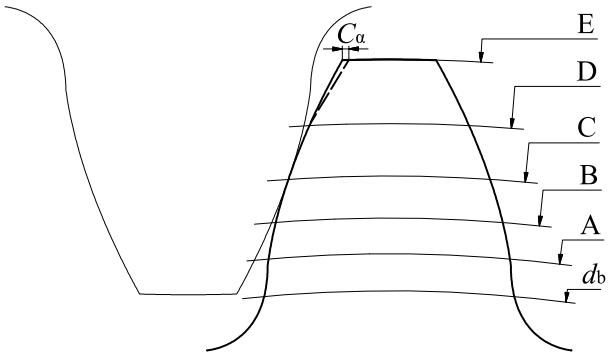

Figure 2: Key gear pair meshing positions

It is also useful to represent gear geometry in terms of roll length or angle of the involute curve. Constant rotation of the gear can be marked as constant intervals of either roll length or angle of the involute. A reminder of the involute geometry of a circle is illustrated in Figure 3. Where r_b is the base radius, φ is

the roll angle of the involute and ρ is the corresponding roll length of the involute. Each position along the involute can be represented in terms of roll length or angle of the involute or radial position, marked r_i, with the reference to the centre of the base circle. The relationship between the two representations can be derived from basic trigonometry and is summarised by the following equation:

$$r_i{}^2 = r_b{}^2 + \rho^2 \qquad for \;\; \{\rho \in \mathbb{R} \mid \rho > 0\} \tag{1}$$

Using a rearranged form of equation (1) and the fact that the radius is half the diameter, key meshing positions from Table 1 can be represented in terms of roll length of the involute. Diametrical or radial dimensions give a better comprehension of the physical size of the gear, however roll length representation is more useful when describing the functionality of the gear. Roll length representation is used later in this paper when presenting measurement results.

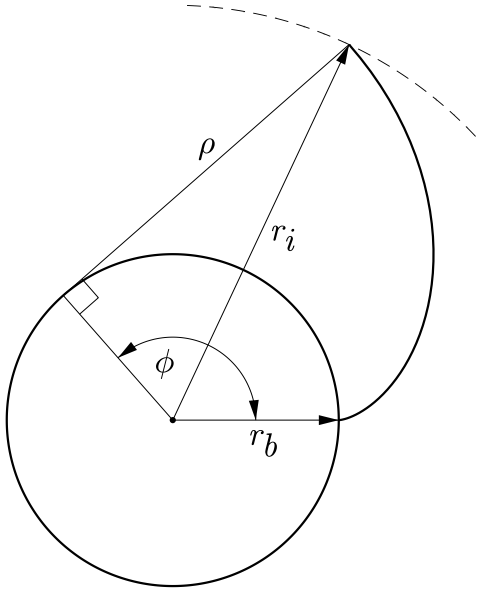

Figure 3: Involute of a circle

2.2 Test rig

Micropitting tests were carried out using 160 mm centre distance back-to-back gear test rig, illustrated in Figure 4 and Figure 5. Mechanical power recirculating back-to-back testing provides efficient full power gearbox testing with the minimal rig operating power. Such a setup consists of two identical test gearboxes (A and B) connected by torsionally compliant shafts in a closed torque loop which allows power recirculation within the system. The torque is induced into the system by a hydraulic torque actuator. This device uses hydraulic pressure to angularly displace a split shaft hence inducing torque into the system. Minimal operating power equivalent to the system loses, such as mesh and bearing friction and oil churning and windage losses, is applied by an external motor through a pulley drive.

Each test gearbox has its own independent lubrication system of 75 L capacity and is equipped with an electric heater and water-cooled heat exchanger. The test rig is equipped with a hydraulic torque actuator with a maximum loading capacity of 6000 Nm, which is applied through a closed loop control system. The test rig is powered by a 45 KW inverter-fed induction motor. Rotational speed of the pulley shaft can be continuously adjusted up to 3000 rpm. The inlet oil temperature, shaft rotation speed and circulating torque are closely monitored and controlled.

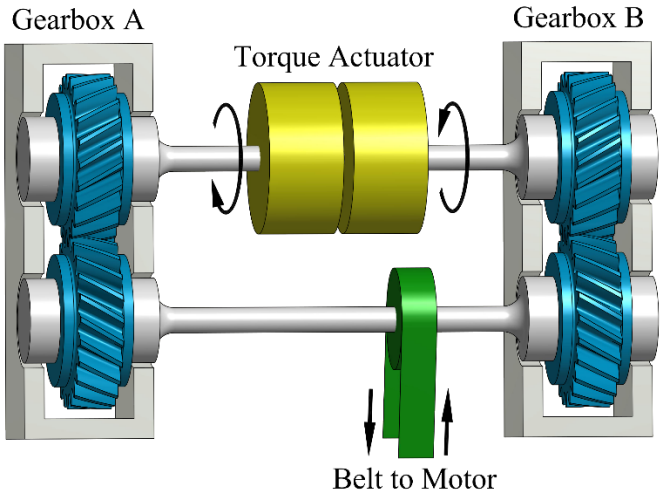

Figure 4: Test rig layout diagram

Figure 5: Test rig photograph

2.3 Test programme

The test programme is divided into three regimes, summarised in Table 2. The first, running in regime, linearly increases the speed and torque applied to the test gears. The objective of this test regime is to let the freshly ground surfaces of the mating gears to conform somewhat which is indicated by plastic deformation and removal of the surface asperities. The load and speed is steadily increased so as to avoid premature failure for example due to scuffing.

The second and third test regimes are conducted at full speed and torque conditions. Stage 1 regime is about a tenth of the stage 2 regime in duration. The goal of stage 1 regime is to initiate some surface degradation. After stage 2 it is expected to observe some further, more serious surface degradation.

Table 2: Test regimes

Test regime	Pinion speed [rpm]	Pinion torque [Nm]	Pinion cycles x10^6
Running in	500 - 3000	250 - 2500	0.302
Stage 1	3000	2500	0.720
Stage 2	3000	2500	7.280

3 Results & discussions

3.1 Roughness measurement & evaluation

Results of a single flank of a wheel gear are presented only for clarity. All of the flanks of the gear pair exhibited similar trends.

Before the beginning of the tests and after each test the chosen gear flank was measured. The nominal involute trace was calculated which provided the ideal form and datum for the measurement. Each of the measured traces were fitted to the nominal involute using least squares point to point fitting algorithm. The form of the nominal involute form was then subtracted from the measured trace, revealing the underlying surface texture features.

The combination of errors resulting from measurement uncertainty and repeatability and the form removal method can produce counter intuitive results. For example certain parts of the after test surfaces are above the as manufactured condition, falsely indicating plus metal condition, as illustrated at the lower end of the measurement length in Figure 6 and Figure 10. However this error is reduced when considering a narrow range and especially in the case of absolute difference of the localised surface texture features, as illustrated in Figure 7, Figure 9 and Figure 11. The authors acknowledge that further improvements to the form removal method can be made.

Low pass Gaussian micro roughness filter with a cut-off wavelength of λ_s = 2.5 µm was used to filter out the noise in the measurement. Additionally a high pass Gaussian long wave filter with a cut-off wavelength of λ_f = 11 mm was used to reduce the residual form errors. The resulting profile of the as manufactured and run in conditions are shown in Figure 6. The form and waviness of the traces could either be genuine surface features or potential errors introduced due to the fitting method. Comparison with a more robust form measurement such as on a GMM, would reveal true form and any fitting errors. However it can be seen that the form for both surface conditions is similar and the difference between the deviation traces reveals localised changes on the surface.

A benefit of using nominal gear form removal is that transformation to gear coordinate system is possible. A secondary horizontal axis in Figure 6 to Figure 11 is used to plot roll length of the gear involute and correspondence to key meshing positions A to E is made.

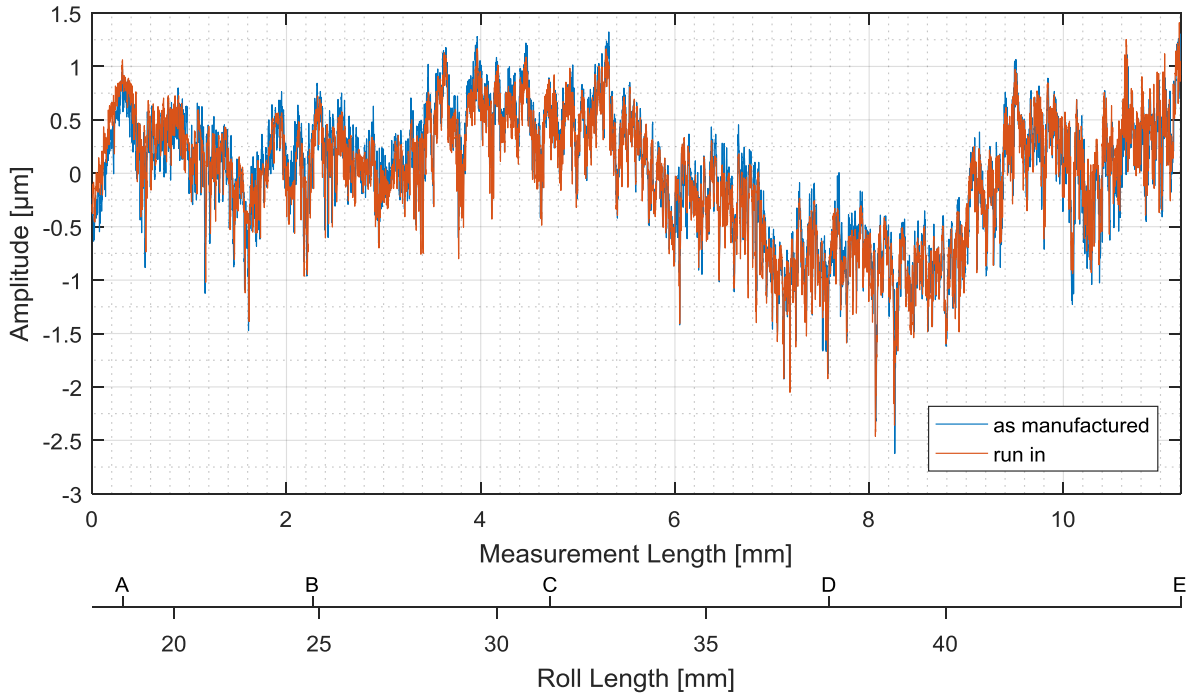

Figure 6: Gear wheel form removed profile, as manufactured and run in conditions.

A magnified range of the traces from Figure 6 is shown in Figure 7. This range is chosen since it exhibits most surface changes after further tests. The range spans key meshing position B, refer to Table 1. This is the position of contact with start of tip relief of the meshing gear and LPSTC. It can be seen that the low cycle running in has reduced peaks by about 0.2 to 0.4 µm.

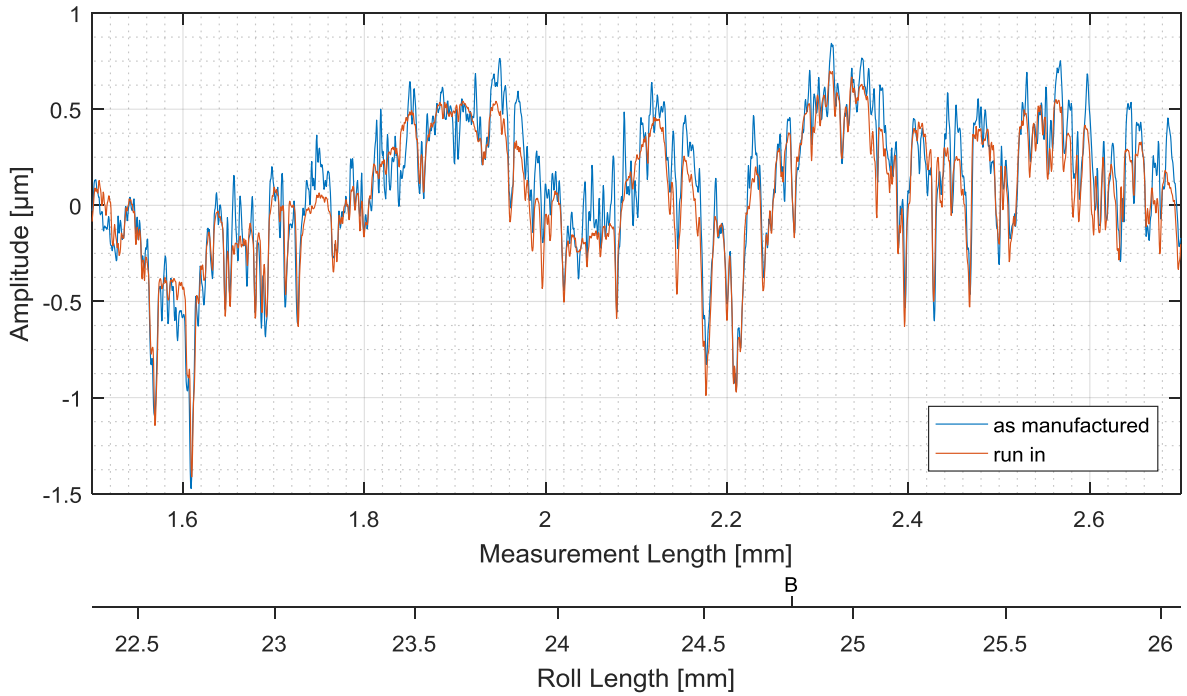

Figure 7: Gear wheel form removed profile, as manufactured and run in conditions. Magnified range. Peak reduction of approximately 0.2 to 0.4 µm.

Form removed and treated profiles of as manufactured and after stage 1 can be seen in Figure 8. The magnified range of the same traces are shown in Figure 9. A slight further reduction of individual peaks can be seen when compared with Figure 7, approximately an additional 0.1 µm. There is also the development of new valleys which indicate micropitting with the largest difference from as manufactured condition of 1.38 µm.

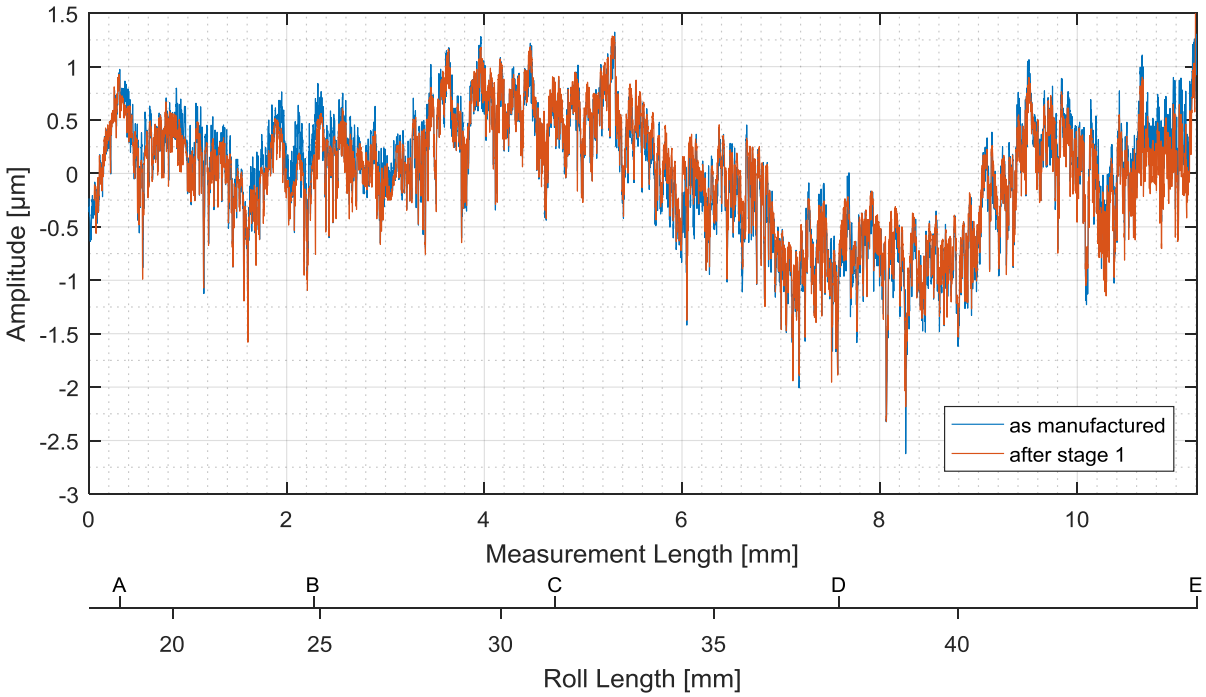

Figure 8: Gear wheel form removed profile, as manufactured and after stage 1 conditions.

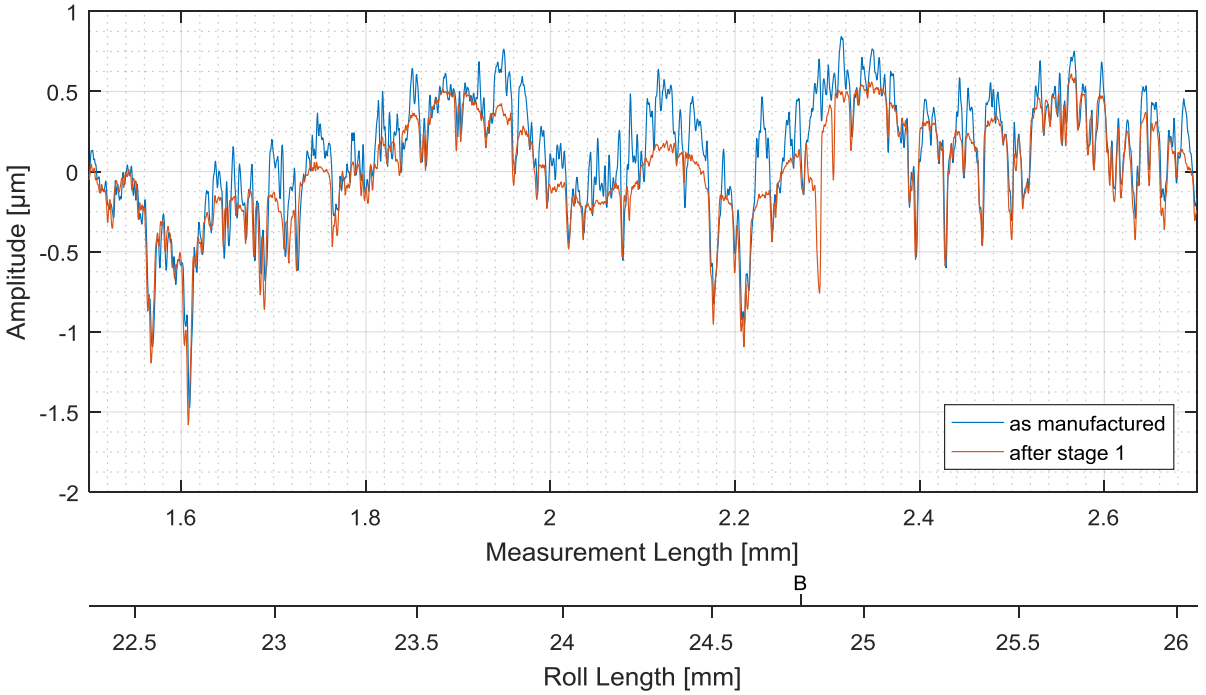

Figure 9: Gear wheel form removed profile, as manufactured and after stage 1 conditions. Magnified range. Peak reduction of approximately 0.2 to 0.5 µm. Maximum difference 1.38 µm between as manufactured trace and biggest valley of the after stage 1 trace, 7 µm wide at the mouth.

Form removed and treated profiles of as manufactured and after stage 2 testing conditions are illustrated in Figure 10. The magnified range of the same traces are shown in Figure 11. New valleys have

developed which indicate micropitting with the largest difference from as manufactured condition of 6.95 µm. It is notable the mouth of this valley is 40 µm wide, therefore the depth of this valley would be significantly attenuated when measured by a GMM with a general stylus tip diameter of 1.5 - 2 mm.

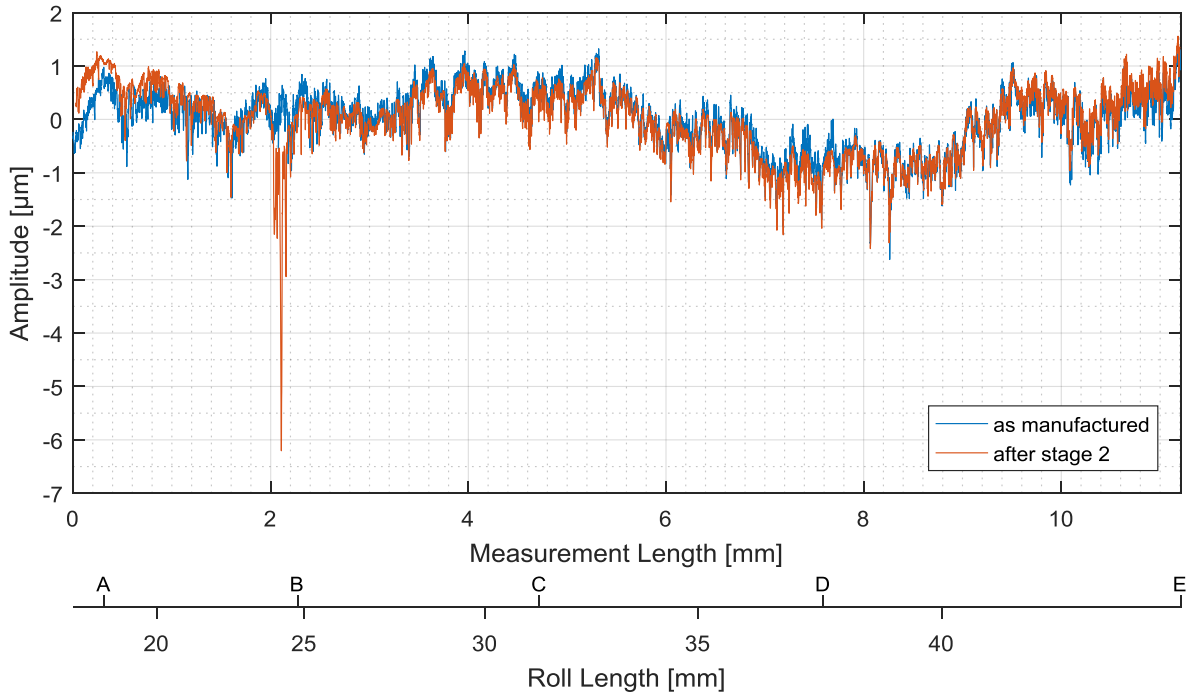

Figure 10: Gear wheel form removed profile, as manufactured and after stage 2 conditions.

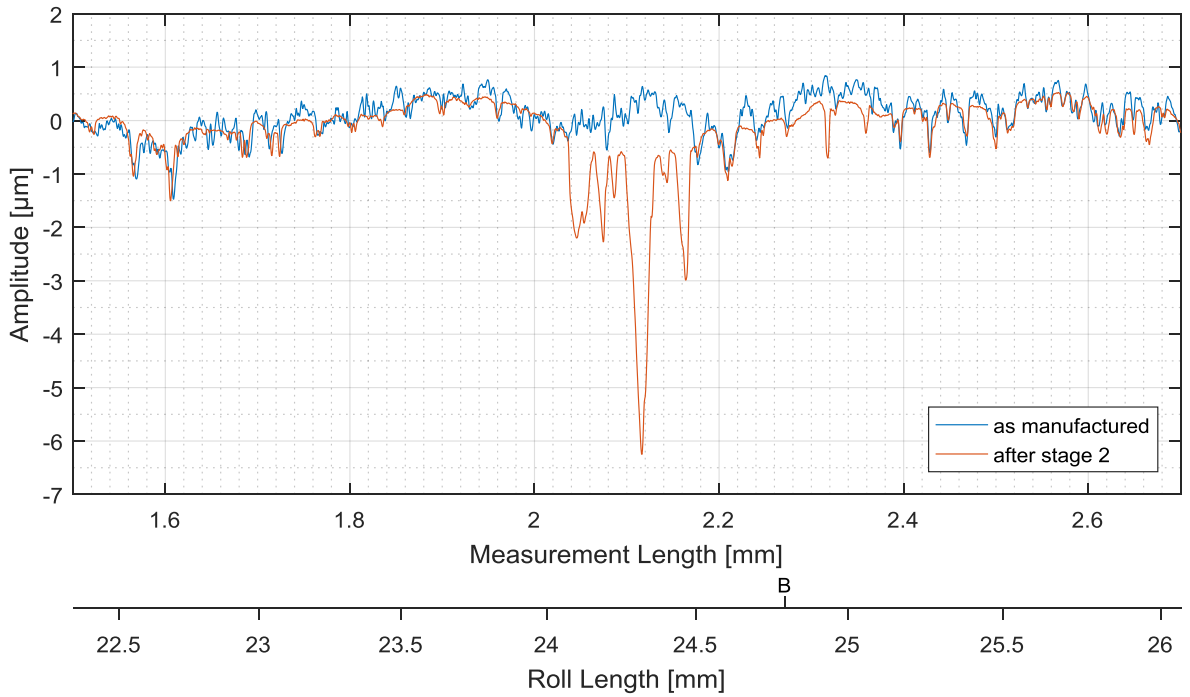

Figure 11: Gear wheel form removed profile, as manufactured and after stage 2 conditions. Magnified range. Maximum difference 6.95 µm between as

manufactured trace and biggest valley of the after stage 2 trace, 40 μm wide at the mouth conditions.

Prior to testing and after each test regime, silicone replication of the gear flank was made to capture the current surface condition. Microscope photographs of the replications are illustrated in Figure 12. An effort has been made to correctly align the replication and capture the range similar to the magnified range in Figure 7, Figure 9 and Figure 11. The x-axis in the photographs approximately correspond to the x-axis measurement length of the profiler trace results. A line drawn horizontally at the y-axis position equals 0 in the photographs, would approximately correspond to the path along which the profiler measurements were taken.

Flattening of the peaks can be observed after running in condition as compared with as manufactured condition, see Figure 12(a) and Figure 12(b). Further flattening of the peaks and development of micropitting can be observed after subsequent testing, see Figure 12(c) and Figure 12(d). It is notable that the position of the area of micropitting on the x-axis seen in the photographs, approximately corresponds to the position of the area of micropitting on x-axis measurement length axis observed in the profiler trace results, compare Figure 12(c) and Figure 12(d) with Figure 9 and Figure 11.

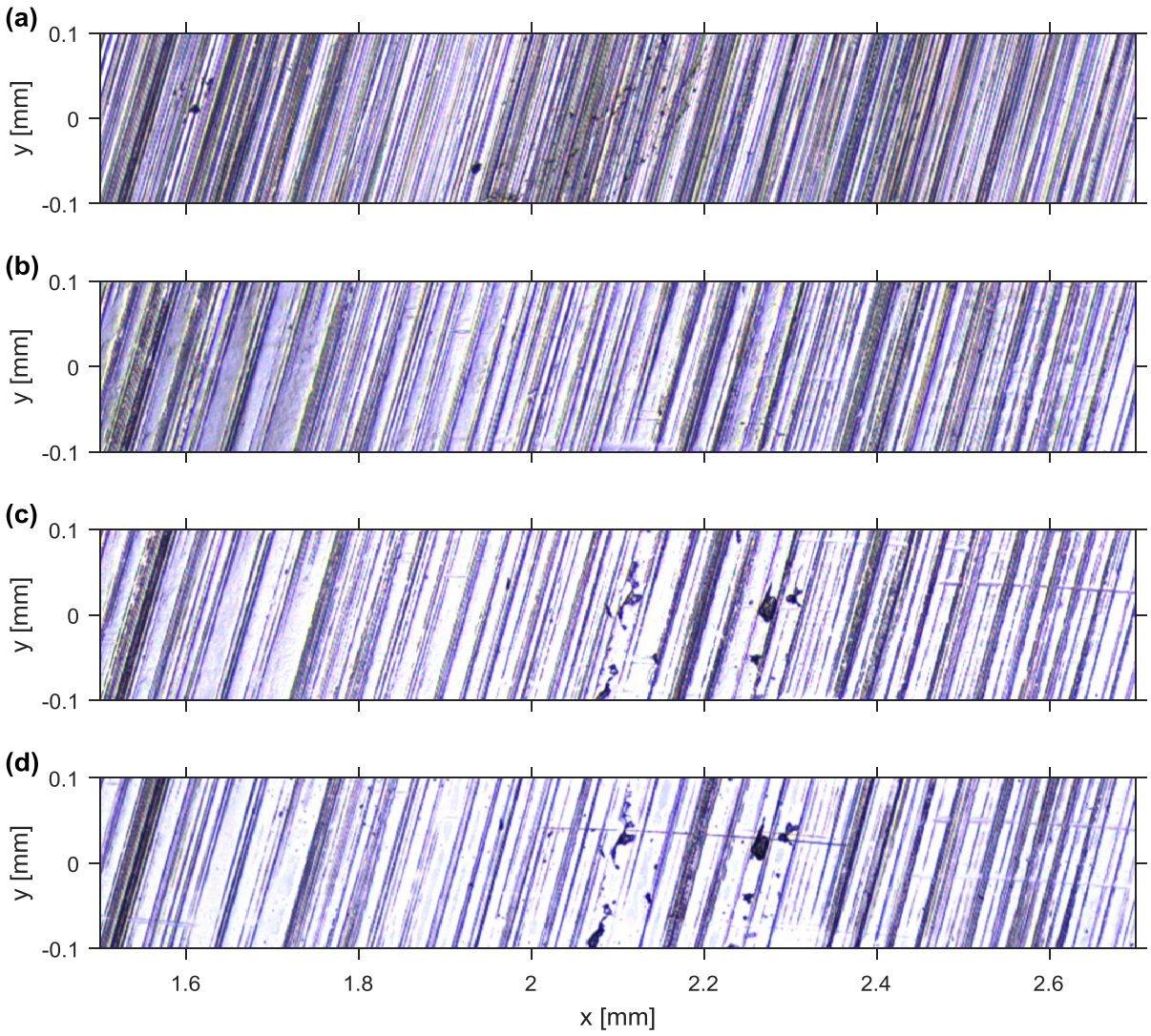

Figure 12: Microscope photograph of the silicone replication of the gear surface (a) as manufactured condition (b) after running in condition (c) after stage 1 condition (d) after stage 2 condition.

The standard roughness measurement analysis was applied to the measurements [10]. A high pass Gaussian long wave filter with a cut-off wavelength of λ_c = 0.8 mm was used to extract the roughness profile. The roughness parameters for the traces considered are summarised in Table 3. Additionally material ratio curve roughness analysis for surfaces with significant pits has been followed [11, 12]. The material ratio parameters are summarised in Table 4. The addendum and dedendum regions of the gear flank are analysed separately, due to their different contact conditions. The major difference being the reversal of the sliding direction at the pitch line. However finer divisions of the flank region is possible in order to resolve finer differences in surface texture.

The magnified range illustrated in Figure 7, Figure 9 and Figure 11 falls into the dedendum region. From Figure 7 the reduction of individual peaks resulting from running in test regime was approximately 0.2 to 0.4 µm. This is reflected by the change in the maximum peak height parameter *Rp*, which is 0.09 µm between dedendum regions (A – C) of as manufactured and run in conditions.

Alternatively a change in the core roughness depth *Rk* and reduced peak height *Rpk* parameters of 0.04 µm and 0.01 µm, respectively is observed for the same region. It would not be expected for core roughness depth to change with the flattening of the peaks, however this could result from the change in the mean line, therefore affecting both core roughness depth and reduced peak height parameters.

Further reduction of individual peaks after stage 1 test regime is shown in Figure 9. Further maximum reduction of approximately 0.1 µm could be observed in the selected range. By comparison the reduction in the parameters *Rp* and *Rk* from run in to after stage 1 condition is 0.03 µm and 0.02 µm, respectively. Creation of new valleys which indicate micropitting was also observed. This is comparable to the increase in valley depth parameter *Rv*. This parameter is reasonably constant between as manufactured and run in conditions reduction of 0.01 µm, which is as expected since no significant new valley development is seen in Figure 7. However in the case of new valleys observed in Figure 9, an increase of parameter *Rv* from dedendum regions (A – C) of as manufactured to after stage 1 of 0.05 µm can be seen. This change has a weak effect on reduced valley depth parameter *Rvk* which reduces from as manufactured to run in conditions by 0.01 µm and again from run in to after stage 1 conditions by 0.01 µm. This could potentially be explained by the localised nature of the newly developed pits which have smaller effect on the parameter *Rvk* which represents the whole region.

Much deeper valleys are seen after stage 2 test regime as shown in Figure 11. This is reflected by the increase in the total height parameter *Rt*. The changes in parameter *Rt* between as manufactured, run in and after stage 1 conditions are small, maximum of about 0.05 µm. This is due to small reduction of peaks and creation of new small valleys. However when comparing dedendum regions (A – C) of as manufactured and after stage 2 conditions an increase in parameter *Rt* from 1.97 to 6.35 µm is seen. This corresponds to the creation of a new region of micropitting with maximum depth of 6.95 µm when compared to the as manufactured condition. Also an increase in parameter *Rvk* of 0.4 µm is observed from as manufactured to after stage 2 conditions. It is notable that material ratio parameters *Rpk* and *Rvk* do not represent the actual peak height and valley depth and therefore are labelled ‘reduced’ in their definition.

Parameters do no always correctly reflect localised change of the surface texture. This is true in cases of parameters with reference to the mean line, since the mean line is changing between the measurement intervals. Additionally average parameters tend to attenuate the effect of the local features.

Table 3: Roughness parameters. Dedendum and addendum regions have been analysed separately, SAP to pitch line (A – C) and pitch line to EAP (C – E).

Condition	Region	*Ra* [µm]	*Rq* [µm]	*Rp* [µm]	*Rv* [µm]	*Rz* [µm]	*Rt* [µm]
as manufactured	A - C	0.22	0.28	0.59	1.15	1.74	1.97
	C - E	0.24	0.31	0.73	1.10	1.83	2.54
run in	A - C	0.21	0.27	0.50	1.14	1.64	1.92
	C - E	0.24	0.30	0.65	1.05	1.70	2.50
after stage 1	A - C	0.20	0.26	0.47	1.20	1.67	2.00
	C - E	0.25	0.32	0.60	1.11	1.71	2.44
after stage 2	A - C	0.25	0.37	0.54	2.02	2.56	6.35
	C - E	0.23	0.30	0.59	1.06	1.64	2.34

Table 4: Material ratio parameters. Dedendum and addendum regions have been analysed separately, SAP to pitch line (A – C) and pitch line to EAP (C – E).

Condition	Region	*Rk* [µm]	*Rpk* [µm]	*Rvk* [µm]	*Mr1* [%]	*Mr2* [%]
as manufactured	A - C	0.67	0.17	0.44	6.7	86.8
	C - E	0.75	0.22	0.43	8.9	87.6
run in	A - C	0.63	0.16	0.45	7.6	86.6
	C - E	0.74	0.18	0.42	7.7	86.7
after stage 1	A - C	0.61	0.16	0.46	7.0	86.1
	C - E	0.79	0.18	0.47	7.0	86.6
after stage 2	A - C	0.62	0.18	0.84	6.9	84.8
	C - E	0.75	0.19	0.43	5.7	87.4

3.2 Key meshing positions

During stage 2 test regime the gear flank has developed a region of new valleys indicating micropitting, see Figure 10 and Figure 11. The use of the nominal involute trace allowed transformation of the measurement length x-axis onto the gear coordinate system in terms of involute roll length. The benefit of such transformation is that correlation to key meshing positions can be drawn. The region indicating micropitting lies closely to key meshing position of LPSTC labelled B which is also the position of contact with start of tip relief of the meshing gear.

Key meshing position B is of significance, since in this region the contact changes from two teeth in contact to a single tooth in contact, in the transverse plane of the gear pair. Additionally, at the same position the contact with start of linear tip relief of the meshing gear occurs. This dynamic change in the gear pair contact manifests itself as an increased contact stress at the contact region. A simulation of the contact using tooth contact analysis (TCA) confirms this. Dontyne Systems Ltd gear simulation software based on the method developed by Haddad [13] and Design Unit, was used. The topography GMM measurement of the test gears in run in condition was used in the TCA. The methodology involving this analysis will be published in the future. The TCA was used to calculate Hertzian contact stress illustrated in Figure 13. It can be seen that the peak stresses are calculated at meshing positions B and D, where maximum damage occurred.

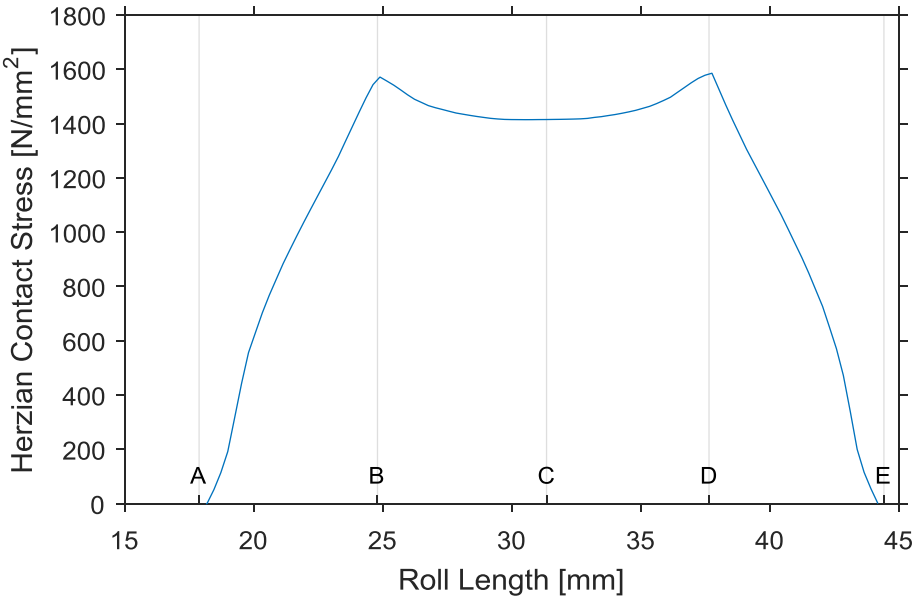

Figure 13: Simulated Hertzian contact stress of the base pitch engagement at the mid face of the meshing gears. Roll length axis has been aligned with the wheel gear.

4 Measurement uncertainty

Uncertainty in the measurement made by the shop floor profiler used for this study has been assessed. The method described in the guide [8] has been followed in part. A type A1 depth measurement calibrated artefact was used to assess the uncertainty in the measurement of vertical displacement. The depth measurement artefact has a flat bottom groove of nominal depth of 1 µm and nominal width of 100 µm. The depth of the groove is comparable with the order of magnitude of the surface texture changes that are expected to be identifiable.

Instrument noise and slide way accuracy were assessed using an optical flat. It was also assumed that the stylus tip will not cause plastic deformation of the measured metal surface larger than 20 nm.

The uncertainty in the measurement of vertical displacement, i.e. z axis U_{TZ} is ±80 nm at 95 % confidence, for displacements between 30 nm and 100 µm.

In order to assess uncertainty in the measurement of spacing roughness parameters, a type C1 sinusoidal roughness measurement calibrated artefact was used. The sine wave profile having *RSm* nominal value of 100 µm and *Ra* nominal value of 0.3 µm. This is representative of the ground gear surface. The approximation method described in the reference [8] yields unrealistic values for average amplitude parameters *Ra* and *Rq*, in some cases values much smaller than the laboratory calibrated values for the artefact. The method suggests that the contribution from the repeatability (standard error of the mean) of the measurement process is taken as the estimate of the uncertainty of these parameters. Therefore to assess the uncertainty in the measurement of amplitude roughness parameters, a simple comparator method was used. The method is summarised by the following equation:

$$u_m = k\sqrt{E^2 + \sigma^2 + {u_c}^2} \quad (2)$$

where u_m is the measurement uncertainty related to the parameter, E is the bias between calibrated value and the mean of the measured value, σ is the standard deviation of the measurement set, u_c is the calibration uncertainty and k is the coverage factor.

Using the comparator method the assessed measurement uncertainties for the amplitude roughness parameters, are summarised in Table 5. The assessment was based on twelve repeat measurements at different positions of the sinusoid roughness artefact. Coverage factor k = 2 was used for 95 % confidence. The assessment of uncertainties for the material ratio parameters could not be carried out due to the lack of appropriately calibrated artefact.

Table 5: Measurement uncertainty of amplitude roughness parameters

Parameter	Mean [µm]	Standard deviation [nm]	Expanded Uncertainty [nm]
Ra	0.31	< 1	±23
Rq	0.35	< 1	±25
Rp	0.53	6	±67
Rv	0.51	7	±61
Rt	1.06	31	±162
Rz	1.03	12	±125

5 Conclusions

A micropitting test was conducted on a pair of test gears. Roughness profile measurements were taken prior to and after each sequential test regime. The measurements were taken following a repeatable well defined gear roughness measurement method published previously [6]. The application of this method has demonstrated the ability to detect sub-micron surface texture changes to a gear flank, despite acknowledging that further improvements to the form removal method is possible. This can be seen in overall surface texture parameters as well as local feature changes.

Application of the measurement method allowed transformation of the arbitrary measurement axis to involute roll length axis inherent to the involute gear geometry. The usefulness of this has been clearly demonstrated. The largest flank degradation was observed near the lowest point of single tooth contact, a key meshing position well defined on the involute length of roll. Highest contact stresses as simulated by TCA correspond with this same position.

The applied roughness measurement evaluation presented in this paper is shown to be useful to gear designers. It was demonstrated that the gear surface texture can be repeatably characterised in reference to the key gear meshing positions. This in turn allows characterisation of the contact fatigue development and perhaps other functional parameters related to gear operation e.g. lubrication condition. The results obtained from this evaluation can be used to form simulation boundary conditions

or to verify models endeavouring to simulate various physical phenomena associated with the gear surface.

Acknowledgements

The authors acknowledge the European Metrology Research Programme (EMRP). The EMRP is jointly funded by the EMRP participating countries within EURAMET and the European Union. This work was completed as part of EMRP collaborative project ENG56.

References

[1] Goch, G., *Gear Metrology*. CIRP Annals - Manufacturing Technology, 2003. **52**(2): p. 659-695.
[2] Zhang, J., *Reducing the Micropitting Wear Rate and Increasing the Micropitting Threshold Stress in Gears*. 2015, Final report of British Gear Association Project 6 Research Consortium. Design Unit.
[3] Staph, H.E., P.M. Ku, and H.J. Carper, *Effect of surface roughness and surface texture on scuffing.* Mechanism and Machine Theory, 1973. **8**(2): p. 197-208.
[4] Fratila, D., *Evaluation of near-dry machining effects on gear milling process efficiency*. Journal of Cleaner Production, 2009. **17**(9): p. 839-845.
[5] Cardoso, N.F.R., et al., *Micropitting performance of nitrided steel gears lubricated with mineral and ester oils.* Tribology International, 2009. **42**(1): p. 77-87.
[6] Koulin, G., et al., *A new profile roughness measurement approach for involute helical gears.* Measurement Science and Technology, 2017. **28**(5): p. 055004.
[7] *PD ISO/TR 15144-1:2014 Calculation of micropitting load capacity of cylindrical spur and helical gears - Part 1: Introduction and basic principles*. 2014, British Standards Institution: London.
[8] Leach, R.K., *Measurement Good Practice Guide No. 37 - The Measurement of Surface Texture using Stylus Instruments*. 2014, National Physical Laboratory: Teddington.
[9] *M3003 The expression of uncertainty and confidence in measurement*. 2012, United Kingdom Accreditation Service: Feltham.
[10] *BS EN ISO 4287:1998 Geometrical product specifications (GPS)–Surface texture: Profile method–Terms, definitions and surface texture parameters*. 1998, British Standards Institution: London.
[11] *BS EN ISO 13565-1:1998 Geometrical product specifications (GPS) – Surface texture: Profile method – Surfaces having stratified functional properties – Part 1: Filtering and general measurement conditions*. 1998, British Standards Institution: London.
[12] *BS EN ISO 13565-2:1998 Geometrical product specifications (GPS) – Surface texture: Profile method – Surfaces having stratified functional properties – Part 2: Height characterization using linear material ratio curve*. 1998, British Standards Institution: London.
[13] Haddad, C.D., *The Elastic Analysis of Load Distribution in Wide-faced Helical Gears*. 1991, Newcastle upon Tyne: University of Newcastle upon Tyne.